JOURNAL OF SOLID STATE CHEMISTRY 93, 403–417 (1991)

Dendritic Surface Morphology of Palladium Hydride Produced by Electrolytic Deposition

PENG JULIN AND L. A. BURSILL

School of Physics, The University of Melbourne, Parkville, Victoria, Australia, 3052

Received December 20, 1990; in revised form March 27, 1991

Conventional and high-resolution electron microscopic studies of electrolytically deposited palladium hydride reveal a fascinating variety of surface profile morphologies. The observations provide direct information concerning the surface structure of palladium electrodes and the mechanism of electrolytic deposition of palladium black. © 1991 Academic Press, Inc.

1. Introduction

Metal hydrides remain of continuing interest to solid state scientists, due to the potential technological importance in fission and fusion reactors, full cells, and energy storage systems (*1*, *2*). Fundamental studies of the interaction of hydrogen with metals was revived recently with the report of meltdown of a Pd–D electrolytic cell (*3*). The Pd–H system has been studied for over a century and it represents a model system from the structural, thermodynamic, and kinetic points of view, due to the high solubility and mobility of hydrogen (also deuterium and tritium) in the face-centered-cubic (f.c.c.) palladium structure. X-ray and neutron diffraction have been used for precision lattice parameter and structural determinations (*2*). Nuclear magnetic resonance, quasielastic neutron scattering, and Mossbauer effect have been used for the study of hydrogen diffusion in palladium (*2*). However, very few, if any, studies have been reported using the technique of high-resolution electron microscopy.

In this paper we present some results of a conventional and high-resolution transmission electron microscopic study of dendritic structures found at the surface of palladium thin foils which had been used as an electrode in an electrolytic cell. The observations, which were quite incidental to our original purpose, provide much stimulating information concerning the surface structure and morphology of palladium electrodes and the mechanism of electrolytic deposition.

The experimental methods and results are first described (Sections 2 and 3). The structural and morphological results are then discussed (Sections 4 and 5).

2. Experimental

Three-millimeter discs were cut from 25-μ thick sheets of high purity palladium metal (99.9%) using an ultrasonic drill. The discs were then thinned electrolytically using a commercial electrochemical jet polishing apparatus. The specimen was used as the anode. The electrolyte was a mixture of 50% CH_3OH, 33% HNO_3, and 17% H_3PO_3. The electrolyte temperature was

0022-4596/91 $3.00

24°C. *V/I* was 2 V/6 mA for 15 min. or until fine pinholes just appeared in the center of the disc, which was then used for electron microscopic observations. H^+ was compressed galvanistically into the prethinned Pd discs described above using as electrolyte a mixture of 5% C_2H_5OH and 50 mol% H_2SO_4 for about 1 hr. The specimen was then made the cathode in the jet electropolisher at room temperature (25°C). The anode was either palladium or platinum foil. *V/I* was 1.5 V/5 mA.

Three samples were prepared using slightly different procedures as follows: (A) electrochemically polished from both sides of the disc; (B) as for A followed by H^+ loading from one side only and (C) H^+ was loaded from both sides of a 25-μm thick disc, which was then electrolytically thinned from both sides. The last preparation was designed to allow us to look for hydride structures in the interior of the Pd foil, i.e., at least 10 μm from the original electrode surface.

The thin specimens were examined in the ultra-high-resolution pole pieces of a JEOL-4000 EX electron microscope, with spherical aberration coefficient C_s = 1.0 mm, equipped with a GATAN electron energy-loss spectrometer with parallel detector (PEELS). The latter allowed us to study the chemical and electronic structure from small volumes of the dendrites, down to ~10 nm diameter.

3. Experimental Results

a. Sample A. The electrochemically thinned disc of palladium showed a clear bright, smooth surface. Dislocations, twins, and stacking faults were common as expected for a f.c.c. metal. Figure 1 is a high-resolution image of a (111) twin boundary viewed along [10$\bar{1}$]. The selected area diffraction patterns (inset Fig. 1) confirm the twin operation across (111). Note that a few stacking faults (extended dislocations) are visible (arrowed in Fig. 1), lying parallel to {111}. Careful annealing and handling of this sample allowed the defects to be reduced to virtually zero.

b. Sample B. This hydrogenated Pd specimen showed the rough, black powdery surface characteristic of palladium black (*4*). Selected area diffraction patterns showed essentially f.c.c. palladium structure. Microcrystallites 100–500 Å in diameter appear at high magnification (Fig. 2a). The high-resolution images (Fig. 2b) contain many stacking faults and defects compared with pure palladium. The surface morphology is also quite different. The f.c.c. crystallites contained dislocations, multiple twins, and stacking faults. The microcrystallites may be aggregated together to produce beautiful dendritic tree patterns for specimens given relatively short hydrogenation treatments (Fig. 3).

Parallel electron energy-loss spectroscopy (PEELS) analysis of microcrystallites from such a tree showed both Pd and H edges ($M_{4,5}$, 334.7 eV for palladium and K_1, 13 eV for hydrogen). We were not able to detect platinum peaks. The absence of the latter implies that there is negligible transfer of metal ions from a platinum anode to the palladium cathode during specimen preparation. Similarly, we were not able to detect oxygen in the dendritic structures, although this is believed to be typically found in palladium black (*5*).

Figures 3a and 3b show a bright-field/dark-field pair of images of a dendritic tree. In another paper we report a fractal analysis of the surface profiles (*6*). The trees have a typical coastline dimension 1.80–1.83, which is in good agreement with a cluster–cluster diffusion-limited aggregation model (D_c = 1.80) (*7*). The selected area diffraction pattern of the whole tree (Fig. 3c) showed that it consists of a mass of palladium black crystallites which are preferentionally oriented with [110] the common direction (parallel to the electron

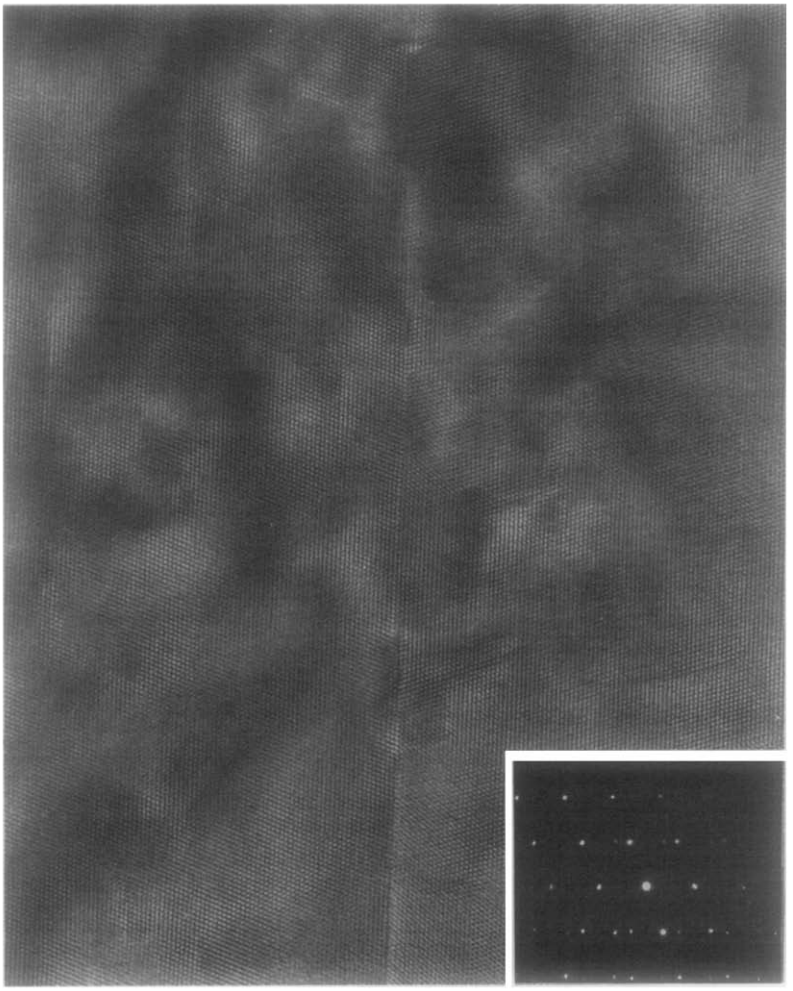

FIG. 1. A high-resolution image of (111) twin boundary in pure palladium viewed along [1$\bar{1}$0]. The selected area diffraction is inset.

beam in Fig. 3c). The spotty ring pattern gave *d*-values consistent with the cell parameters of palladium metal (a = 3.90 Å). A selected area diffraction pattern from three parallel leafs of one branch of the tree (shown and enlarged in Fig. 3e) is given as Fig. 3d. This shows the leaves to be aligned almost exactly parallel to each other, with [110] common. The almost perfect alignment of the microcrystallites parallel to [110] may also be deduced by comparison of the bright-field/dark-field pairs of images (Figs. 3a,b) which show almost perfect contrast reversal. Part of a high-resolution image is inset as Fig. 3f. Further enlarged images of dendrite branches are given in Figs. 3g–3h, showing how the microcrystallites aggregate together. Note the preferential alignment of defects within adjacent microcrystallites in Fig. 3g.

Figures 4a–4c give high-resolution lattice images, showing fine detail of the internal

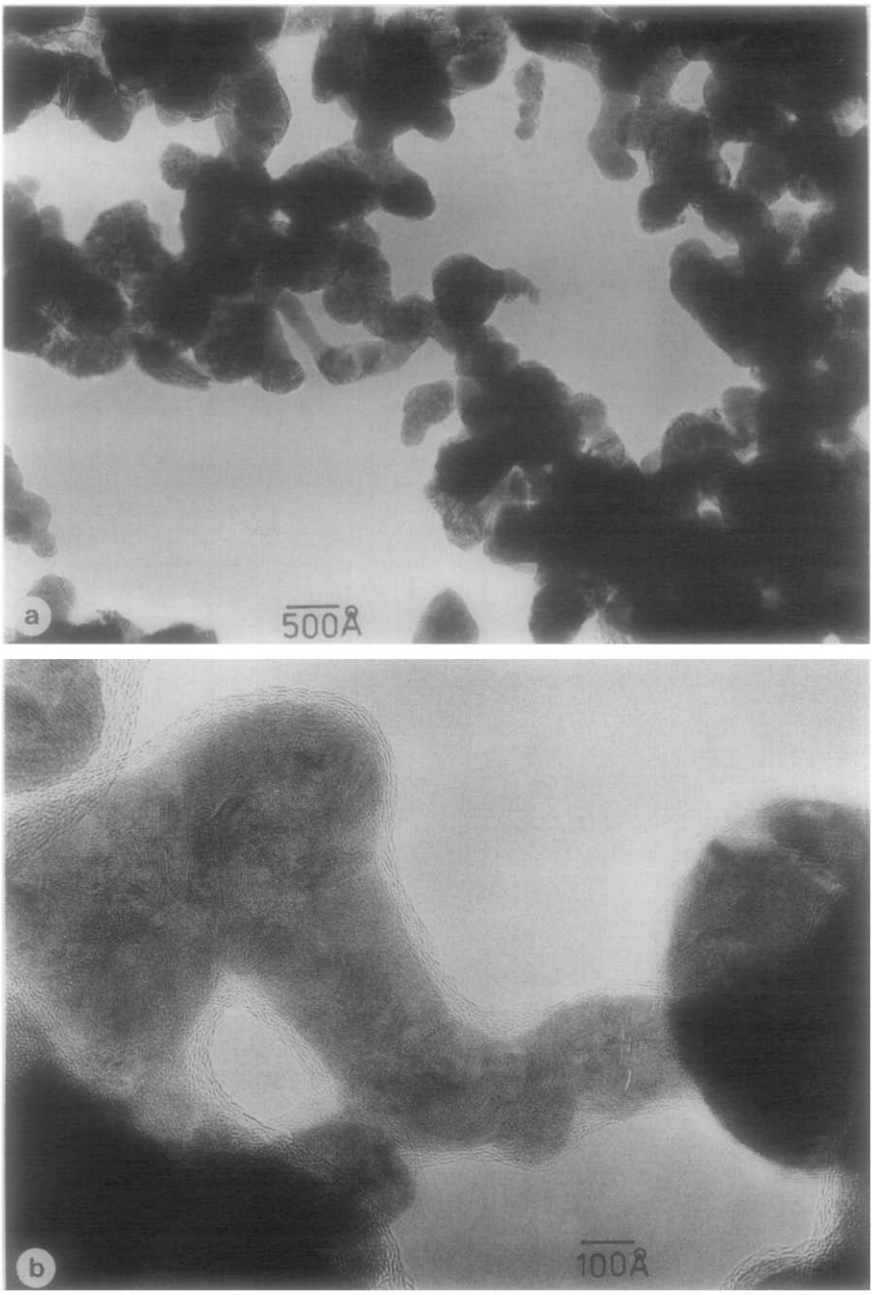

FIG. 2. (a) Rough surface of sample B (palladium black) shows microcrystallites 100–500 Å diameter and (b) high-resolution image showing detail of the surface morphology.

structure and interfaces between microcrystals. Complex twinning and intergrowth structures appear, and the surface morphology is convoluted. Some of the crystallites are roughly circular in profile but most have irregular shape. The high density of microtwins and lamellae intergrowth defects suggests that these are associated with the electrolytic hydrogenation process, either to relieve mechanical stress due to hydrogen occupying octahedral sites in the palladium (see discussion below, Sections 4 and 5) or else providing direct access to hydrogen via a chemical diffusion mechanism, with the hydrogen incorporated in the defects (cf. chemical twinning (*8*)). The twinning may be parallel (Fig. 4b) or rotational (Fig. 2d) giving rise to multiply twinned particles. Figure 4c shows an area where microcrystallites joined the palladium substrate. The latter contains many short defects lying on {111} planes. Both the twins and the stacking faults lie parallel to {111} type planes. Note the fringe shift of certain lattice planes on crossing stacking faults (sight along the lattice rows in Fig. 4c). Note that the stacking fault density increases with increasing specimen thickness.

Figure 5 gives a series of surface profile images, showing different stages of development of the surface morphology. Isolated dendrites (Fig. 5a) give way to impinging dendrites (Fig. 5b), which then tend to coarsen (Fig. 5c) and finally take more facetted crystallographic shapes which tend to pack together along the surface (Fig. 5d). In the latter two stages the surface profile tends to show a quasiperiodic character. This sequence corresponds to increasing electrolysis time. A self-affine fractal analysis has been carried out of this process (see (*6*) for details).

c. Sample C. After the rough palladium black surfaces were polished away a smooth, clean bright surface again appeared. These specimens showed a high density of short line contrast defects, parallel to {111} type planes of palladium. These were always associated with dislocations or stacking faults (Fig. 6a). High-resolution images reveal dilational-type strain fields corresponding to the tail of the dislocations (Figs. 6b and 6c), suggesting that the stacking faults are extrinsic.

4. Structure of Internal Defects

Palladium has the f.c.c. structure with cube edge $a = 3.890$ Å. Figure 7 shows a perspective view of the unit cell, showing the positions of the atoms (a) and the octahedral and tetrahedral interstices, emphasized by drawing nearest-neighbor bonds in (b). There are twice as many tetrahedral as there are octahedral sites. Using the close-packed layer description (*9*) f.c.c. palladium may be represented by the stacking sequence ABCABC. . . . By reversing the normal alternation of atomic planes we obtain a mirror symmetry configuration; i.e., a twin. Thus the sequence ABC ↓ BAC . . . represents a (111) mirror twin boundary (the arrow denotes the position of the twin composition plane.

Twins and stacking faults as discussed above may be introduced by plastic mechanical deformation of palladium, e.g., by bending or cold working of the original palladium foil. However, the relatively high density of defects in specimen B relative to specimen A implies that diffusion of hydrogen, and possibly oxygen to a lesser extent, into the metal may produce an expanded structure ($a' > a$). Hydrogen is known to occupy octahedral interstices (*10*), causing an increase in the average cell parameter.

It seems to us that the observed defects probably include hydrogen-induced stacking faults as well as oxygen-induced nonstoichiometric intergrowth defects. Both hydrogen and oxygen dissolution should occur preferentially in association with stacking faults and microtwin lamellae

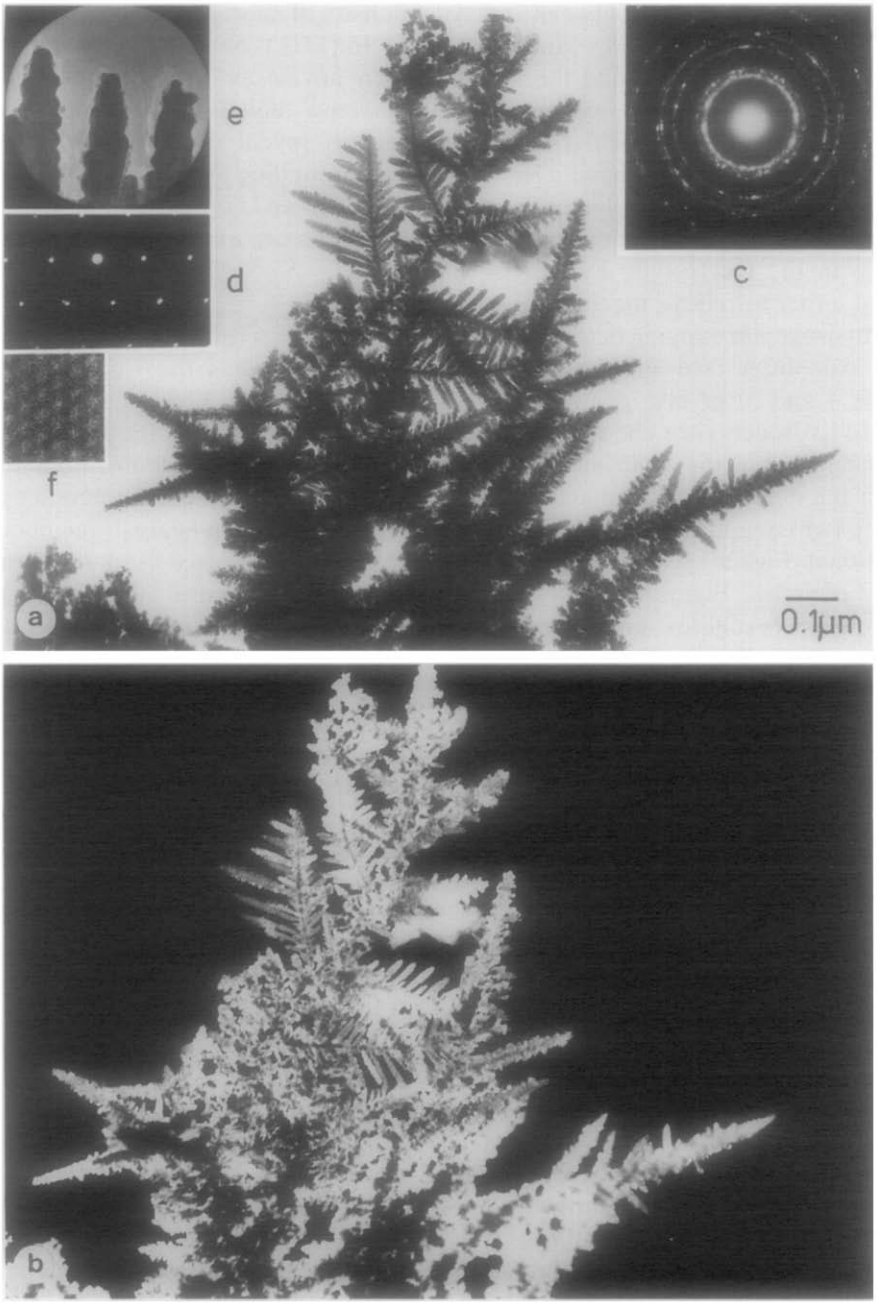

FIG. 3. (a,b) A bright-field/dark-field pair of images of a dendritic tree (palladium black). (c) Selected area diffraction pattern of (a), showing spotty-ring pattern of f.c.c. crystallites with preferential orientation [110]. (d) Selected area diffraction pattern from three parallel branches (circled in (a)), showing simple [110] zone spot pattern. (e) Enlargement of area contributing to (d). (f) Part of a high-resolution image. (g, h) are high magnification images showing various ways the microcrystallites are aggregated together. Note alignment of defects in adjacent microcrystallites.

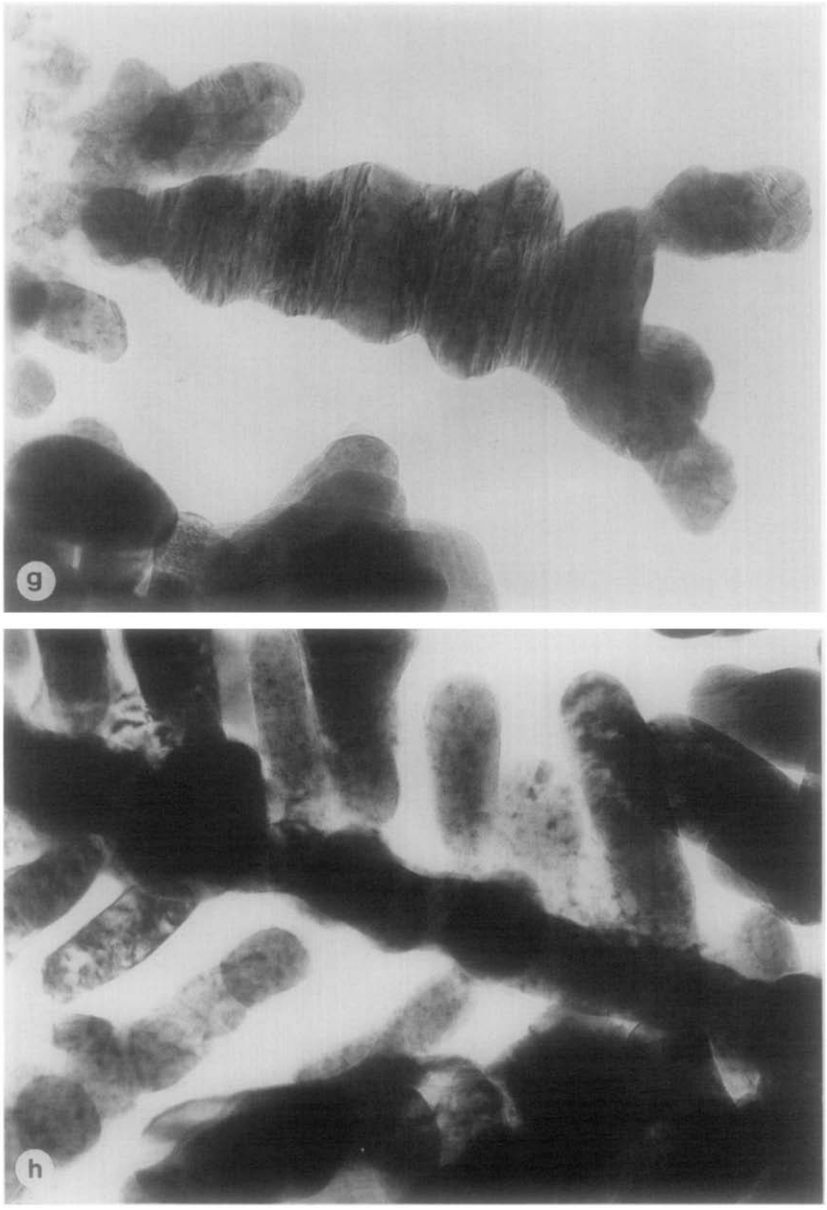

which exist in the palladium prior to electrolysis. Oxygen, as well as hydrogen, should be readily available, due to absorbed water or ethanol molecules from the electrolyte.

The observation of multiply twinned microcrystallites (Fig. 2b) and other features of the dendritic structures shows clearly that there is a complex process occurring at the electrode surface, involving both partial

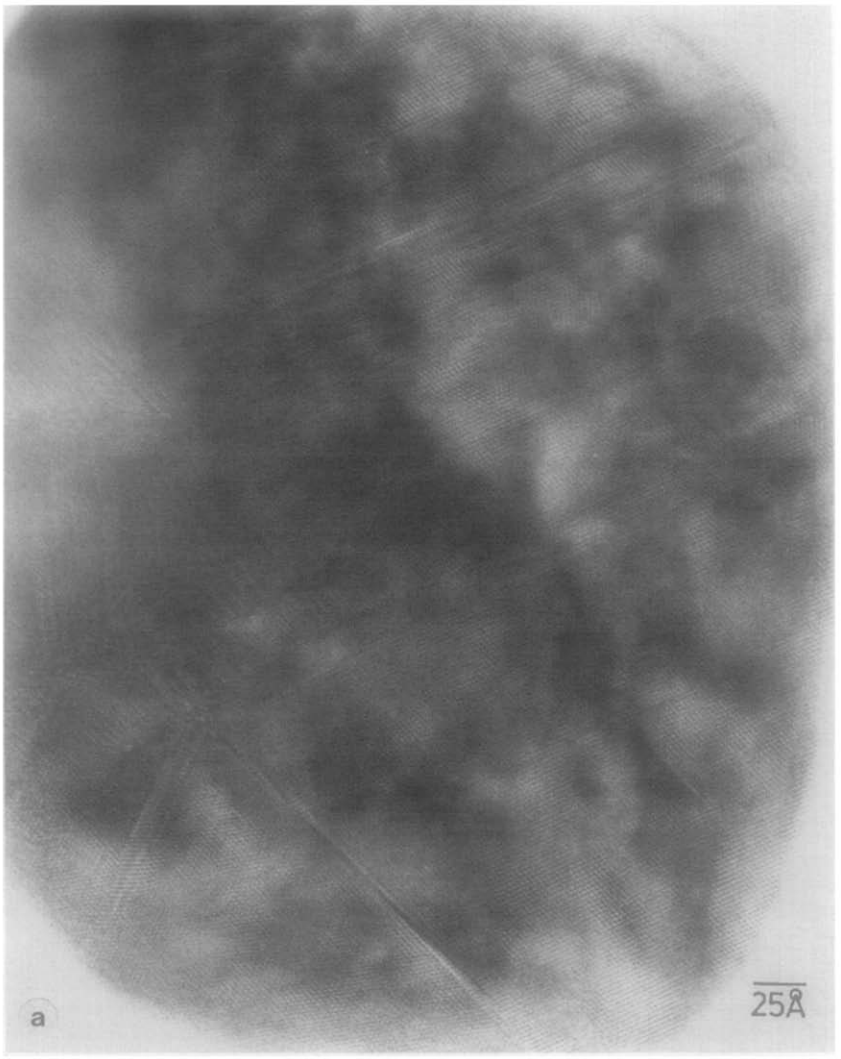

FIG. 4. (a–c) Fine detail of intergrowth defects and interfaces of palladium black. Note small defects in (c).

dissolution and deposition mechanisms. This will be discussed in the next section. The high-resolution images are used for atomic structure modelling and computer simulation.

5. Discussion of Electrode Reactions

Essentially we are concerned here with the cathodic dissociation of H_2O to produce active hydrogen (H^+) and its simultaneous absorption into the metallic cathode. The instability of the Pd electrode surface, characterized by the growth of three-dimensional dendrites, must be associated with the electrolytic reaction. The observed morphology requires simultaneous electrodissolution and electrocrystallization processes. These highly defective structures provide irrigation channels for the migra-

FIG. 4—*Continued*

tion of chemiadsorbed hydrogen atoms. Internal defects (stacking faults, partial dislocations, intergrowth defects, lamellae twinning, and multiple-twinning) presumably provide local paths for enhanced diffusion of hydrogen, and possibly oxygen.

The process of dendritic growth of palladium black particles on the Pd cathode has been described as a multistep, recurrence electrodereaction (5). Contributions to dendritic growth may involve both cathodic and anodic reactions. The reader is referred to (5) for a statement of fairly modern theories of electrochemistry.

Electrodeposition involves a surface diffusion process in two or three dimensions. It contains some of the elements of a random growth process, but it is further controlled by the electric field (external source), which obeys Laplace's equation.

FIG. 4—*Continued*

Computer simulation of the formation of dendritic growths, and the changeover to a coarsening growth mechanism (see Fig. 5) was achieved by Vicsek (*12*). An elementary theory of dendrite formation is presented next, for its physical understanding. The reader is referred to Ref. (*12–16*) for recent reviews of fractal approaches to heterogeneous chemistry and fractal growth phenomena.

a. Classical theory of dendrite formation. Suppose that a macrospiral growth develops on a flat Pd surface. The tip of the spiral may have a small radius of curvature (approximately a few nm) (Fig. 8). This is virtually a point sink with a radius of curva-

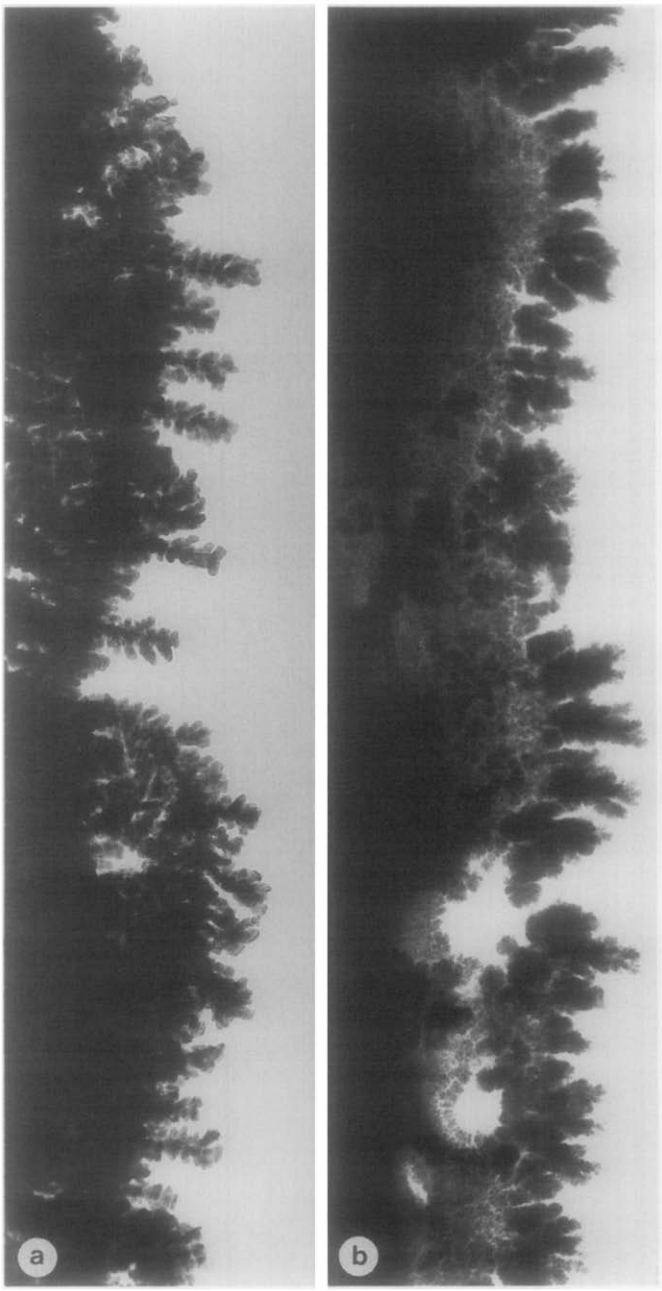

FIG. 5. Series of four surface profiles for increasing electrolysis periods. Note isolated dendrite trees (a), impinging trees (b), coarsening (c), and development of quasiperiodic compacted crystallites in (d).

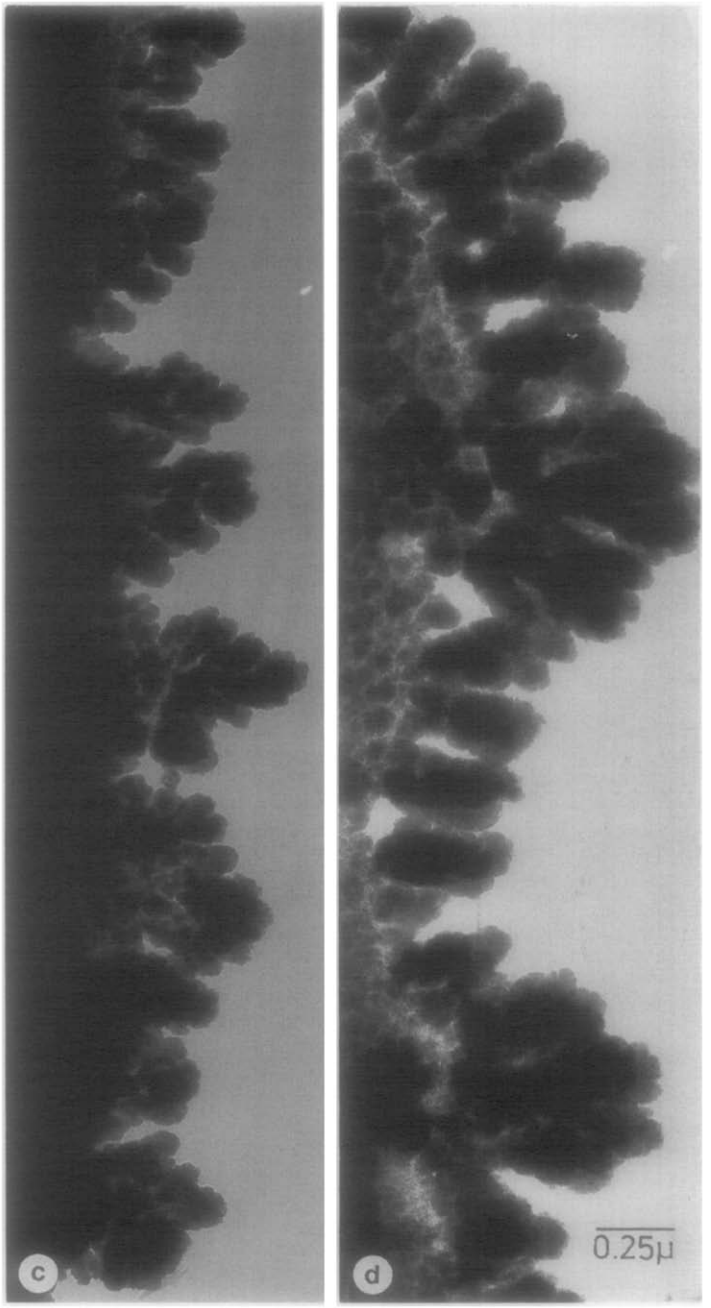

FIG. 5—*Continued*

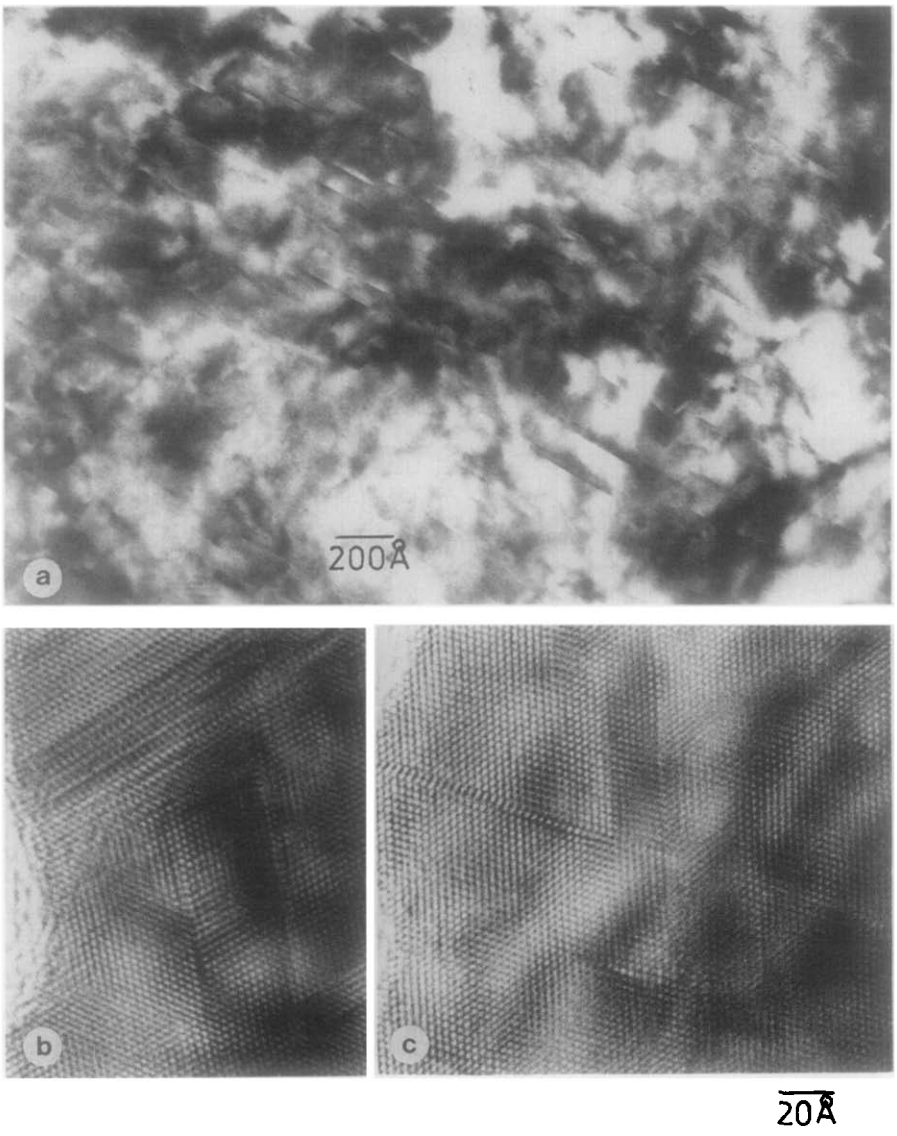

FIG. 6. Low (a) and high-resolution images (b, c) of small planar defects (stacking faults/partial dislocations) in Sample C (bulk hydrided palladium).

ture much less than the diffusion layer thickness ($r \ll \delta$). Under these conditions there is spherical diffusion to the point sink, and the limiting current density is proportional to $1/r$ rather than to $1/\delta$, which is the case for linear or planar diffusion (*5*). Since $r \ll \delta$, it is obvious that the limiting current density to the spiral tip is much higher than to a protuberance with a radius of curvature equal to the diffusion layer thickness. It follows, therefore, that electrogrowth tends to become concentrated at the spiral tip. The tip tends to grow faster than the rest of the substrate. This is part of the basis of the

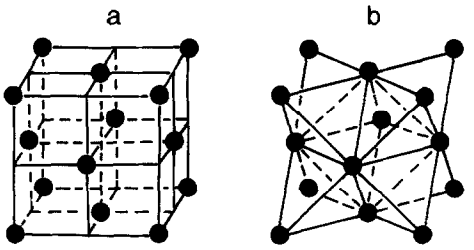

FIG. 7. The f.c.c. structure of Pd highlighting a perspective view of the unit cell (a) and the octahedral and tetrahedral interstices (b).

theory of the growth of long, thin, fast-growing facetted rods, which sometimes shoot out from the electrode surface. These dendrites usually grow side arms, ending up like fir trees (Fig. 3).

b. Hydrogen transfer catalysts. The transfer of hydrogen from the electrolyte into the Pd crystal structure comprises two steps. (I) The dissociative chemisorption of hydrogen molecules at the Pd surface and (II) the passage of hydrogen atoms from surface sites into the lattice

$$\text{I} \quad H_2^s \rightleftarrows 2H_{ads}$$
$$\text{II} \quad H_{ads} \rightleftarrows H_{metal} \tag{5}$$

Absorbed hydrogen atoms, which can get desorbed in either a chemical or an electrodic reaction as hydrogen molecules, may diffuse out into the solution as gas bubbles.

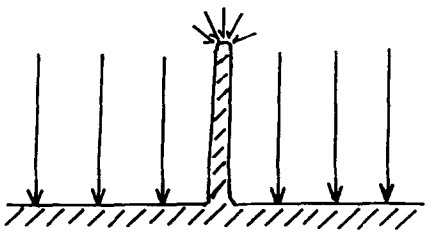

FIG. 8. Representation of the elementary dendrite theory. The tip of a macrospiral has radius of curvature $r \ll \delta$ (diffusion length) and hence the growth rate is much greater at the tip than on a flat surface.

This is a visible desorption of hydrogen. There is also a route for hydrogen into the surface. Thus adsorbed hydrogen atoms can dissolve into the metal. Since one has started off with zero concentration of adsorbed hydrogen inside the bulk of the metal, a gradient of hydrogen concentration develops from the surface to the interior. This gradient will tend to drive hydrogen to diffuse into the metal. Thus the dendritic growths plays an important role in hydrogen transfer catalysis, greatly increasing the active surface area on which active dissociation of H occurs. The hydrogen atoms from the catalyst surface spill over to the Pd surface and they enter the lattice. The twins, stacking faults, and partial dislocations provide irrigation channels for the diffusing hydrogen. Hydrogen will also diffuse through the lattice interstitial sites, e.g., octahedral sites, but grain boundaries and cracks will offer lower resistance to diffusion. It may not be an exaggeration to suggest that the *dendritic surfaces* act as a "hydrogen transfer catalyst" reservoir.

c. Trapping of hydrogen. When a hydrogen atom enters the palladium lattice there may be a certain displacement of the surrounding atoms, to accommodate the hydrogen interstitial atom. This feeds through to an overall increase in average cell parameter, with the dilation increasing according to the hydrogen content. All the lattice imperfections will also tend to dilate the crystal with respect to the original ideal f.c.c. structure (*10*). Hence adsorbed hydrogen will first tend to locate at lattice imperfections and grain boundaries. The more rapid diffusion of hydrogen takes precedence over the diffusion of oxygen, also being driven by the higher chemical potential for formation of PdH compared to PdO. The major extended defects in bulk palladium are the partial dislocations shown in Fig. 4, which will presumably trap hydrogen in the dilatation strain field of the partial, which extends for ~13–40 Å. Shockley and Frank

negative dislocations correspond to insertion of an extra plane (extrinsic stacking faults). We expect that the hydrogen solubility in palladium at room temperature may be considerably enhanced by increasing the dislocation densities by plastic deformation.

d. Practical effects of dendrites. In energy storage devices (batteries) dendrites often rupture the membranes which separate the electrodes. They may finally cause short-circuits and battery failure. In electrodeposition processes designed for the production of metal powders, dendrite formation is to be avoided because it leads to particles of undesirable size and packing density. Dendritic surfaces may also increase electrocatalytic reactions and the electrical capacitance of the electrical double layer, i.e., the interface between the electrode and the electrolyte due to the enhanced surface area effect. It may be that electrical energy, stored due to the (presumeably) large capacitance of the dendritic structures of palladium black, may contribute to some of the effects observed by Fleischmann and Pons (*3*).

6. Conclusions

It is clear that the combination of conventional and high-resolution electron microscopy, applied to surface profile morphology, provides a powerful approach to the characterization of electrolytically deposited surfaces. Taken together with appropriate analysis of the scaling properties (i.e., coastline and self-affine fractal analyses: see Refs. (*6, 12*)) it should be possible to characterize different stages of the disorderly growth processes involved. High-resolution studies of the internal defects due to hydrogen absorption are in preparation. The approaches referred to above should be applicable to a wide range of electrolytically deposited materials. Chemical information, using energy-dispersive X-ray and/or parallel electron energy-loss spectroscopic techniques, should also be available at high spatial resolution.

Acknowledgments

This work was supported financially by the Australian Research Council and The University of Melbourne. We are grateful for the technical support of Mr. David Dryden.

References

1. L. Wood and A. J. Jones (Eds.), "New Developments in Electrode Materials and their Applications," Department of Industry, Technology and Commerce, Canberra, Australia (1990).
2. G. Alefeld and J. Völkl "Topics in Applied Physics, Vols. 28 and 29, Hydrogen in Metals," Vols. I and II, Springer, Berlin (1978).
3. M. Fleischmann and S. Pons, *J. Electrochem. Soc.* **210,** 301 (1989).
4. J. F. Lynch and T. B. Flanagan, *J. Phys. Chem.* **77,** 2628 (1973).
5. J. O'M. Bockris and A. K. N. Reddy, "Modern Electrochemistry," Vols. 1 and 2, Plenum, New York (1977).
6. L. A. Bursill, Peng JuLin, and Fan XuDong, *Int. J. Mod. Phys. B.*, in press. (1991).
7. P. Meakin "Phase Transitions," Vol. 12, pp. 335–498 Academic Press, New York (1988).
8. L. A. Bursill and Peng JuLin. *Philos. Mag A* **46,** 1 (1982).
9. W. L. Bragg and G. F. Claringbold "Crystal Structures of Minerals," G. Bell, London (1965).
10. Ch. A. Wert, *in* "Topics in Applied Physics, Vol. 28, Hydrogen in Metals, Vol. I. Basic Properties," Springer, Berlin (1978).
11. G. M. Clark, "The Structures of Non Molecular Solids," Applied Science Publishers, London (1972).
12. T. Vicsek, *Phys. Rev. Lett.* **53,** 2281 (1984).
13. R. Jullien and R. Botet, "Aggregation and Fractal Aggregets," World Scientific, Singapore (1987).
14. D. Grier, E. Ben-Jacob, R. Clarke, and L. M. Sander, *Phys. Rev. Lett.* **56,** 1264 (1986).
15. D. Avnir (Ed.), "The Fractal Approach to Heterogeneous Chemistry," Wiley, New York (1989).
16. T. Vicsek, "Fractal Growth Phenonema," World Scientific, Singapore (1989).